JOURNAL OF
AGRICULTURAL AND FOOD CHEMISTRY

Modeling Evaluation of Carbaryl Degradation in a Continuously Stirred Tank Reactor by Anodic Fenton Treatment

LINGJUN KONG AND ANN T. LEMLEY*

Graduate Field of Environmental Toxicology, TXA, MVR Hall, Cornell University, Ithaca, New York 14853-4401

Anodic Fenton treatment (AFT) has been shown to be effective in removing pesticides from aqueous solution in batch reactors with the formation of less toxic and more biodegradable products. To facilitate practical application of AFT, carbaryl degradation in a continuously stirred tank reactor (CSTR) by AFT was investigated under different experimental conditions, such as carbaryl inlet concentration, Fenton reagent concentration/ratio, and carbaryl feeding flow rate. A higher Fe^{2+} delivery rate and H_2O_2 to Fe^{2+} ratio (H_2O_2:Fe^{2+}) were found to favor the carbaryl degradation process, whereas flow rate was shown to be a much less significant factor to influence the degradation rate under the evaluated experimental conditions. A kinetic-based semiempirical model was developed to simulate the experimental data, and a very good fit between the model and the raw data was found ($R^2 >$ 0.99). A dimensionless parameter (k/q^2) was found to be a good indicator of the degradation rate; that is, the higher the k/q^2 value is, the faster the degradation process is. The rate parameter (k) can be used to evaluate the degradation rate when the flow rate is invariant for a given pesticide. The shape parameter (β) is most likely related to the availability and reactivity of Fenton reagents and hydroxyl radicals. To compare the degradation rate of different pesticides, more information other than k/q^2, k, and β values, such as the instantaneous degradation rate vs time relationship, needs to be considered.

KEYWORDS: Carbaryl; pesticides; degradation; CSTR; Fenton reaction; kinetics

INTRODUCTION

With the fast development of agriculture, the use of pesticides has increased over the past 50 years in order to achieve high yields and quality of crops. As a result of the heavy application of pesticides, we have had to face the serious problems generated by pesticide wastes, which could eventually endanger the water resources and human health (*1, 2*). As toxic chemicals, pesticides could enter the aquatic ecosystem by manufacturing industry wastewater, rinsewater of pesticide containers or application equipments, incidental spills or leakage, or improper disposal. Therefore, the treatment of pesticide wastewater generated by manufacturing industry or agriculture related activities has been the focus of researchers and regulators (*3–5*).

Numerous techniques including physical, chemical, photochemical, thermal, and microbiological treatments have been studied and employed for the disposal of pesticide wastewater. Most of the treatment technologies have been investigated in batch reactors (*6–9*), while much less has been investigated in continuous-flow reactors, such as continuously stirred tank reactors (CSTR) and plug-flow reactors (*3, 5, 10*). From the perspective of large-scale practical use, continuous reactors are usually more effective both operationally and economically.

The Fenton and modified Fenton treatment, which generates hydroxyl radicals (•OH) through decomposition of hydrogen peroxide (H_2O_2) in the presence of catalysts [such as Fe(II), Fe(III), Mn(II), and Mn(IV)], is one of the most extensively used chemical oxidation processes in pesticide wastewater treatment (*11, 12*). The hydroxyl radical (•OH) is a powerful and nonspecific oxidant, which has been widely accepted as the major intermediate capable of degrading a wide range of organic compounds at a near diffusion-controlled rate (10^9–10^{10} M^{-1} s^{-1}) (*13*). However, as with all of the other wastewater treatment processes, chemical oxidation has its shortcomings. For example, chemical oxidation can lead to the production of even more persistent or toxic products. Therefore, the selection of the most effective and environmentally friendly process is essential in pesticide wastewater treatment.

Anodic Fenton treatment (AFT) based on the Fenton reaction degrades pesticides in a batch reactor by using electrogenerated ferrous ion (Fe^{2+}) as shown in eqs 1 and 2:

$$\text{anode: } Fe \rightarrow Fe^{2+} + 2e \quad (1)$$

$$\text{cathode: } 2H_2O + 2e \rightarrow H_2 + 2OH^- \quad (2)$$
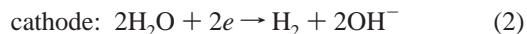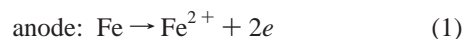
This method overcomes the disadvantage of handling easily oxidized ferrous salts. In addition, the application of the anion exchange membrane, which can prevent the H^+ from passing

* To whom correspondence should be addressed. Tel: 607-255-3151. Fax: 607-255-1093. E-mail: ATL2@cornell.edu.

through the membrane and being reduced at the cathode, enables the pH of the anodic solution to remain below 3. AFT has shown great potential in pesticide wastewater treatment and is reported to be capable of removing >99% of many pesticides, such as 2,4-D, carbamate, carbofuran, diazinon, and metribuzin, among others, from aqueous systems within 10 min (*7−9, 14−16*). The AFT degradation products have been found to become more biodegradable as evidenced by an increase in the 5 day biochemical oxygen demand to chemical oxygen demand ratio (BOD$_5$/COD) to >0.3, indicating a completely biodegradable solution (*17, 18*). In other work, a toxicity assay shows that the fatal toxicity of carbofuran to earthworms can be totally removed after the AFT process (*16*).

For the purpose of better evaluating the efficiency of various pesticide degradation technologies and optimizing the operating conditions, the kinetics of pesticide degradation have been widely investigated. Kinetic modeling can typically be classified into two main categories: reaction mechanism/kinetic-based modeling and mathematical function-based modeling. The first approach starts with the mechanisms and kinetics of various reactions occurring in the evaluated system and ultimately reaches a relationship between the dependent variable (i.e., pesticide concentration) and the independent variable (i.e., time) and various reaction parameters (i.e., reaction rate constants) (*5, 7, 19, 20*). The mathematical model is developed by simulating the obtained experimental data to typical mathematical functions such as polynomial, exponential, Weibull, etc. and interpreting the physical meaning of each fitting parameter (*6, 21*). The advantage of the reaction mechanism-based modeling is that it can interpret the physical meaning of each parameter quite well. In a well-defined simple system, under some reasonable assumptions and simplifications, a very informative expression can be obtained. For example, the AFT kinetic model developed by Wang and Lemley (*7*) has been shown to describe the pesticide degradation in a batch reactor by AFT very well, with regression coefficient (*R*) values >0.99. However, in most cases, the reaction mechanisms and kinetics are not well understood, which hinders the development of kinetic models. In addition, the resulting differential equation based on well-defined reaction kinetics can become very complicated, making it impossible to obtain an analytical solution and requiring a numerical solution (*5, 19*). As for the mathematical function-based modeling approach, even if one could find a function to fit the experimental data very well, it is always challenging to interpret the physical meaning of each fitting parameter. In addition, it is difficult to describe the raw data by a simple mathematical function in many cases.

The purpose of this study is to apply AFT to the removal of pesticides in a CSTR and develop a kinetic-based model to evaluate the degradation process and optimize the treatment conditions. Carbaryl (1-naphthyl N-methylcarbamate), a carbamate insecticide, was selected as a representative target compound. The specific objectives of this research are to (i) develop a model based on reaction kinetics to simulate the pesticide degradation process and validate this model; (ii) examine the effects of various experimental conditions such as carbaryl inlet concentration, Fenton reagent delivery rate/ratio, and carbaryl feeding flow rate on the carbaryl degradation process; and (iii) employ the developed kinetic model to evaluate the degradation of other pesticides, such as alachlor, carbofuran, diazinon, metolachlor, and 2,4-D, in CSTR by AFT.

MATERIALS AND METHODS

Chemicals. 2,4-D, carbaryl, carbofuran, diazinon, and hydrogen peroxide (30%) were purchased from Sigma-Aldrich Chemicals (Milwaukee, WI). Alachlor and metolachlor were purchased from Chem
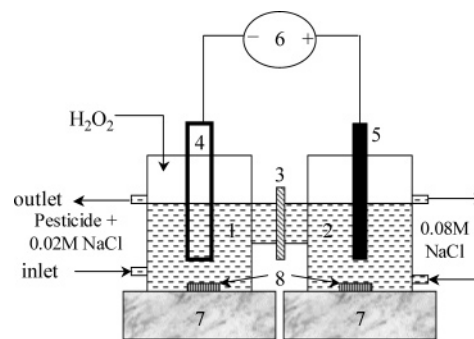

Figure 1. AFT apparatus: 1, anodic half-cell; 2, cathodic half-cell; 3, anion exchange membrane; 4, iron plate; 5, graphite rod; 6, DC power supply; 7, magnetic stirring plate; and 8, magnetic stir bar.

Service (Chester, PA). Acetonitrile [high-performance liquid chromatography (HPLC) grade], ammonium acetate buffer, hydroxylamine hydrochloride (10%), methanol, *o*-phenanthroline (0.1%), phosphoric acid (85%), sodium chloride, and water (HPLC grade) were purchased from Fisher Scientific (Fair Lawn, NY). Iron stand solution (10 ± 0.1 mg L^{-1}) was obtained from HACH company (Loveland, CO). All reagents used were certified grade except where specifically indicated. Deionized water (DI water) was obtained from a Barnstead Nanopure system with an electric resistance of the effluent water >18.1 MΩ cm^{-1}. All solutions were prepared from DI water.

Degradation of Pesticides in CSTR by AFT. The AFT apparatus (**Figure 1**) consisted of two 150 mL customized glass half-cells (anodic and cathodic half-cell) separated by an anion exchange membrane (Electrosynthesis, Lancaster, NY) with an electric resistance of 8 Ω cm^{-2} in 1 M NaCl. A pure iron plate (2 cm × 10 cm × 0.2 cm) and a graphite rod [1 cm (i.d.) × 10 cm (length)] were used as the anode and cathode, respectively. The electric current (*I*) was supplied by a BK Precision DC power supply 1610. The pesticide solution with a NaCl concentration of 0.02 M was fed into the anodic half-cell by a Carter Cassette pump (Manostat, Division of Barnant Company) at a given flow rate, and the effluent was collected in a waste bottle. The outlet was set at a given height to keep the volume of the solution in the cell approximately 90 mL. Because the electrolyte solution in the cathodic half-cell was very stable for at least an hour, in most of the conducted experiments, approximately 90 mL of 0.08 M NaCl solution was added to the cathodic half-cell without continuously feeding and discharging. The solution in each half-cell was mixed by a magnetic stirring bar during the AFT process. Hydrogen peroxide was delivered into the anodic half-cell using a Stepdos peristaltic pump (Chemglass Inc., Vineland, NJ) at a flow rate of 0.50 mL min^{-1}. Unless specified otherwise, the electric current was kept at 0.020 A, and the corresponding H$_2$O$_2$ concentration was 0.062 M, which resulted in an H$_2$O$_2$ to Fe^{2+} delivery ratio (H$_2$O$_2$:Fe^{2+}) of 5:1. The DC power supply was turned on, and the electric current was adjusted to a certain value once the first drop of hydrogen peroxide entered the pesticide solution in the anodic half-cell. Over a given time period, 1.0 mL of pesticide solution was taken out by a 1000 μL Eppendorf micropipetter at certain time intervals and transferred immediately to a 1.5 mL HPLC vial containing 0.1 mL of methanol, which served as a quencher of hydroxyl radicals. The collected pesticide solution was hand-shaken and ready for pesticide concentration analysis. All experiments were performed at room temperature (22.0 ± 1.0 °C). Each treatment was repeated three times. Control experiments of carbaryl degradation were conducted for three cases: (i) in the absence of both Fenton reagents (Fe^{2+} and H$_2$O$_2$), (ii) in the presence of Fe^{2+} but the absence of H$_2$O$_2$, and (iii) in the presence of H$_2$O$_2$ but the absence of Fe^{2+}. Each control experiment was also conducted in triplicate.

Concentration Analysis of Pesticides, Ferrous Ion, and Hydrogen Peroxide. The pesticide concentration was analyzed by a reverse-phase HPLC system equipped with a Restek ultra C18 (5 μm) column (4.6 mm × 150 mm) and a diode array (DAD) UV/vis detector (Series 1100, Agilent Technology). The DAD wavelength was chosen at 280 ± 20 mm. The mobile phase consisted of acetonitrile and water with an acetonitrile:water ratio of 60:40 for carbaryl and 2,4-D, 65:35 for

Table 1. Summary of Major Chemical Reactions Involving Fenton-like Treatment

reactions	rate constant, k_i (M^{-1} s^{-1})	refs
$Fe^{2+} + H_2O_2 \rightarrow Fe^{3+} + {}^{\bullet}OH + OH^-$	53–76	25
$Fe^{3+} + H_2O_2 \rightarrow Fe^{2+} + {}^{\bullet}O_2^- + OH^-$	$2 \times 10{-}3$	13
$Fe^{3+} + {}^{\bullet}O_2^- \rightarrow Fe^{2+} + O_2$	2.0×106 (pH3.0)	26
$Fe^{2+} + {}^{\bullet}OH \rightarrow Fe^{3+} + OH^-$	$2.3{-}5 \times 108$	27
${}^{\bullet}OH + H_2O_2 \rightarrow HO_2^{\bullet} + H_2O$	2.7×107	13
$HO_2^{\bullet} + Fe^{2+} \rightarrow HO_2^- + Fe^{3+}$	1.2×106	13
$2{}^{\bullet}OH \rightarrow H_2O_2$	5.2×109	28
${}^{\bullet}OH + HCO_3^- \rightarrow CO_3^{2-} + H_2O$	8.5×106	13
${}^{\bullet}OH + organics \rightarrow products$	108–1010	13

alachlor, carbofuran, and metolachlor, and 70:30 for diazinon. The pH of the water phase was adjusted to 3.0 using phosphoric acid. The retention times of alachlor, carbaryl, carbofuran, diazinon, metolachlor, and 2,4-D under the described analytical conditions were 9.2, 6.0, 4.1, 10.6, 9.9, and 5.0 min, respectively.

The ferrous ion concentration was analyzed by using the phenanthroline method (*22*). The hydrogen peroxide concentration was determined by potassium permanganate titration (*23*). The sample collection was similar to that of pesticide degradation products.

Experimental Data Analysis. All of the figures and statistical analyses were completed using SigmaPlot 9.01 (*24*).

RESULTS AND DISCUSSION

Development of a Kinetic-Based Model of Pesticide Degradation in a CSTR by AFT. The mass balance of chemical species in a CSTR can be expressed as:

$$V\frac{dC}{dt} = QC_0 - QC + rV \tag{3}$$

where C and C_0 are the outlet and inlet concentrations of the chemical species (μM), respectively, V is the volume of solution in the CSTR (mL), Q is the fluid flow rate in and out of the reactor (mL min^{-1}), r is reaction rate of the chemicals (μM min^{-1}), and t is the time (min).

Assuming that q is the reciprocal of the hydraulic retention time (min^{-1}) ($q = Q/V$), eq 3 becomes

$$\frac{dC}{dt} = qC_0 - qC + r \tag{4}$$

Considering the continuous delivery and generation/consumption of ferrous ion (Fe^{2+}) in the AFT system, reactions kinetics involving Fe^{2+} are difficult to express in a simple function (**Table 1**) (*13, 25–28*). For the purpose of simplification, we assume that the net input and generation/consumption of Fe^{2+} is ϵv_0, where ϵ is a parameter related to the average lifetime of Fe^{2+} in the reactor and v_0 is the Fe^{2+} delivery rate (μM min^{-1}). Therefore, the ferrous ion concentration ($[Fe^{2+}]$) can be obtained by solving eq 5, an expression of the mass balance of $[Fe^{2+}]$:

$$\frac{d[Fe^{2+}]}{dt} = \epsilon v_0 - q[Fe^{2+}] \tag{5}$$

which is,

$$[Fe^{2+}] = \frac{\epsilon v_0}{q}[1 - \exp(-qt)] \tag{6}$$

Similarly, we define ϕ as the constant related to the H_2O_2:Fe^{2+} delivery ratio and the H_2O_2 consumption ratio. The mass balance of H_2O_2 in the CSTR can be expressed as:

$$\frac{d[H_2O_2]}{dt} = \phi v_0 - q[H_2O_2] \tag{7}$$

Therefore,

$$[H_2O_2] = \frac{\phi v_0}{q}[1 - \exp(-qt)] \tag{8}$$

As discussed in the previously developed batch AFT model, the rate constant for the ${}^{\bullet}OH$ reaction ($10^7–10^{10}$ M^{-1} s^{-1}) is several orders of magnitude faster than that of the Fenton reaction ($\sim$76 M^{-1} s^{-1}). Thus, the Fenton reaction can be considered as the controlling step in the AFT process. Therefore, the instantaneous concentration of hydroxyl radicals ($[{}^{\bullet}OH]$) can be assumed to be proportional to its generation rate for a constant hydroxyl radical sink, which is true in the evaluated AFT system (*7*).

$$[{}^{\bullet}OH] = \lambda\frac{d[{}^{\bullet}OH]}{dt} = \lambda k_1[Fe^{2+}][H_2O_2] \tag{9}$$

where λ is the average lifetime of ${}^{\bullet}OH$ (min) and k_1 is the Fenton reaction rate constant (μM^{-1} min^{-1}).

Substituting eqs 6 and 8 into 9 yields

$$[{}^{\bullet}OH] = \frac{\lambda k_1 \epsilon \phi v_0^2}{q^2}[1 - \exp(-qt)]^2 \tag{10}$$

Therefore, the pesticide reaction rate can be obtained as follows:

$$r = -k_2[{}^{\bullet}OH]C = -\frac{\lambda k_1 k_2 \epsilon \phi v_0^2}{q^2}[1 - \exp(-qt)]^2 C =$$
$$-\frac{k}{q^2}[1 - \exp(-qt)]^2 C \tag{11}$$

where k_2 is the second-order rate constant of pesticide reacting with ${}^{\bullet}OH$ (μM^{-1} min^{-1}) and k is a reaction rate parameter ($k = \lambda k_1 k_2 \epsilon \phi v_0^2$) (min^{-2}).

Substituting eq 11 into eq 3 yields the governing equation of pesticide degradation in a CSTR by AFT:

$$\frac{dC}{dt} = qC_0 - qC - \frac{k}{q^2}[1 - \exp(-qt)]^2 C \tag{12}$$

Validation and Modification of the Developed Model. To validate the developed model (eq 12), the instantaneous concentrations of Fe^{2+} and H_2O_2 were measured at H_2O_2:Fe^{2+} ratios of 2:1, 5:1, and 10:1. Equations 5 and 7 were found to give poor simulation to the measured Fe^{2+} and H_2O_2 concentration profiles (simulation not shown). However, modified expressions of instantaneous concentration of Fe^{2+} and H_2O_2 better fit the experimental data:

$$[Fe^{2+}] = \frac{\epsilon v_0}{q}[1 - \exp(-qt)]^{\beta_1} \tag{13}$$

$$[H_2O_2] = \frac{\phi v_0}{q}[1 - \exp(-qt)]^{\beta_2} \tag{14}$$

where β_1 and β_2 are parameters most likely related to the reactivity and availability of the Fenton reagents and hydroxyl radicals.

Simulations using the modified functions (eqs 13 and 14) gave better fits to the measured concentration profiles. To show the raw data and model simulation more clearly, concentration
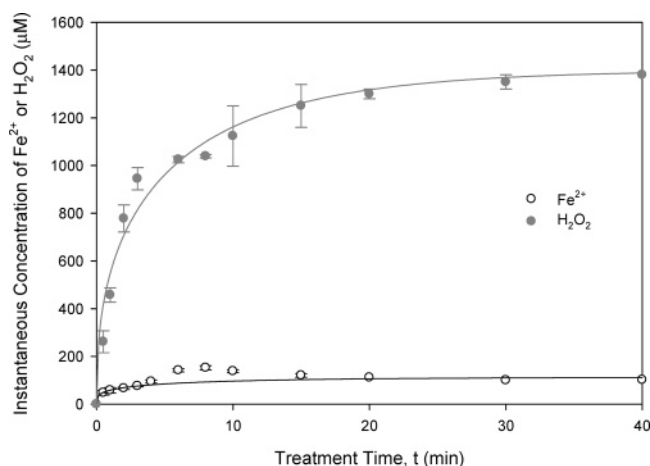
10064 *J. Agric. Food Chem.,* Vol. 54, No. 26, 2006

Kong and Lemley

Figure 2. Instantaneous concentration profile of Fenton reagent (Fe^{2+} and H_2O_2) at H_2O_2:Fe^{2+} delivery ratios of 5:1 in CSRT by AFT [carbaryl inlet concentration (C_0) = 100.50 μM, I = 0.02 A, and Q = 7.5 mL min^{-1}] (symbols represent experimental data and lines represent fitting curves).

profiles of Fe^{2+} and H_2O_2 at a H_2O_2:Fe^{2+} ratio of 5:1, which is the typical ratio used in the presented research, are illustrated in **Figure 2**. The Fe^{2+} concentration deviates from a smooth curve during the initial stage of treatment ($\sim$5$-$10 min), most likely caused by known or unknown reactions involving Fe^{2+}. However, the modified function (eq 13) fits the overall Fe^{2+} concentration curve fairly well. Similarly, the other modified expression (eq 14) provides an even better prediction of the H_2O_2 concentration ($R^2 > 0.96$).

Considering the complex and uncertain interactions between the reactive species and the intermediates (i.e., Fe^{2+}, H_2O_2, $\cdot$OH, etc.), it is reasonable to simplify the intermediate variables in an effort to produce a solvable final differential equation without losing the consistency between the model and the experimental data. On the basis of the adjusted expressions for Fe^{2+} and H_2O_2 concentrations, the developed governing equation of pesticide degradation in CSTR by AFT (eq 12) can be modified as:

$$\frac{dC}{dt} = qC_0 - qC - \frac{k}{q^2}[1 - \exp(-qt)]^{2\beta} C \quad (15)$$

where β is defined as the shape parameter, which is related to the reactivity and availability of the Fenton reagents and hydroxyl radicals. The magnitude of β is proportional to $\beta_1 + \beta_2$. This differential equation (eq 15) is called the kinetic-based semiempirical model of pesticide degradation in CSTR by AFT and can be solved numerically by using the fourth-order Runge$-$Kutta method in SigmaPlot 9.01.

Effect of Carbaryl Inlet Concentration on Its Degradation. Carbaryl degradation in CSTR by AFT was investigated at five inlet concentration levels (C_0) (20.52, 40.45, 60.02, 79.66, and 99.75 μM) with other experimental conditions fixed at I = 0.020 A, H_2O_2:Fe^{2+} = 5:1, and a carbaryl feeding rate Q = 10.0 mL min^{-1}. The pH of the pesticide solution dropped quickly from the original pH (5.6) to approximately 3.0 within 2 min and stayed below 3.0 during the entire AFT process. Control experiments showed no sorption of carbaryl on the wall of the reactor and no reduction of carbaryl at the anode. At the same time, no carbaryl degradation was observed in the absence of both or either of the Fenton reagents. In the AFT degradation experiments, carbaryl was not detected in the reactor within 10 min for all five inlet concentrations (**Figure 3a**). The higher the inlet concentration is, the longer the treatment time needed
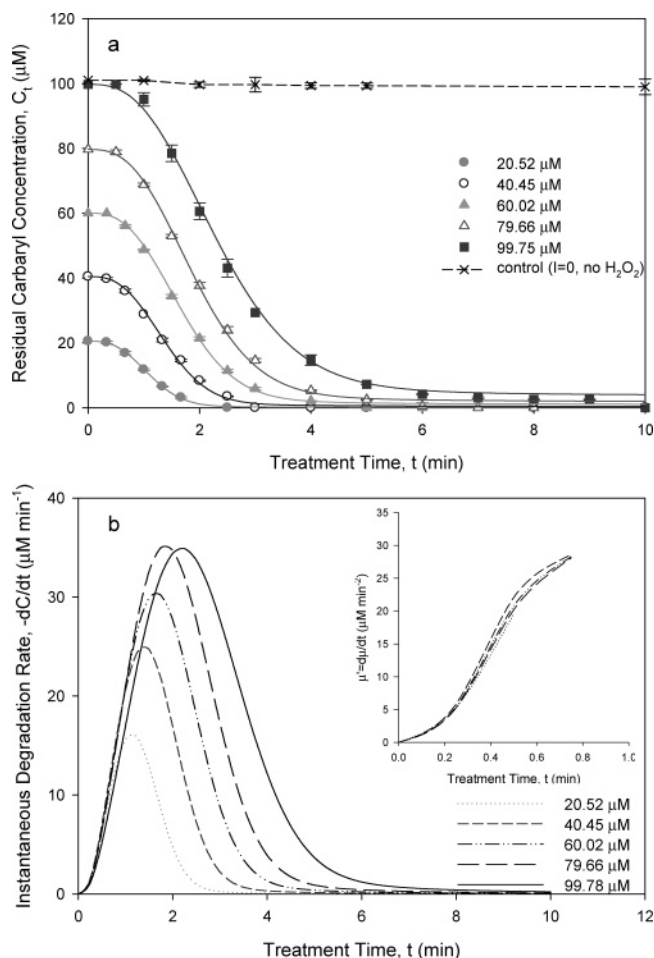

Figure 3. Effect of carbaryl inlet concentrations (C_0) on its degradation in CSRT by AFT (I = 0.02 A, H_2O_2:Fe^{2+} = 5:1, and Q = 10.0 mL min^{-1}). (**a**) Modeling fit of experimental data (symbols represent experimental data, and lines represent model fit). (**b**) Model predicted instantaneous degradation rate as a function of treatment time; the inset is the dμ/dt vs treatment time curve.

Table 2. Modeling of Carbaryl Degradation under Different Inlet Concentrations in CSTR by AFT

inlet concn, C_0 (mM)	k (min^{-2})	β	R^2	half-life of carbaryl, $t_{1/2}$ (min)
20.52	0.629 ± 0.008	0.79 ± 0.01	1.000	1.08
40.45	0.350 ± 0.008	0.80 ± 0.01	0.998	1.38
60.02	0.218 ± 0.008	0.79 ± 0.01	0.999	1.66
79.66	0.159 ± 0.004	0.80 ± 0.01	0.998	1.90
99.51	0.099 ± 0.002	0.80 ± 0.01	0.998	2.35

to achieve near complete degradation is. A similar trend was observed in our laboratory during 2,4-D degradation with different initial concentrations in a batch reactor by AFT (7).

When fitting the observed experimental data to the developed kinetic-based model in the previous section (eq 15), the reaction rate parameter (k) and the shape parameter (β) were determined by comparing the model-predicted carbaryl concentration at a given time to the corresponding experimental data to achieve the highest value of R^2, which is considered the best fit. The fitted parameters (k and β) and R^2 values are listed in **Table 2**. On the basis of the obtained k and β values, the model-predicted carbaryl concentration profiles were compared to experimental data and a very good fit was observed ($R^2 \geq 0.998$) as shown in **Figure 3a**. The reaction rate parameter k increases from 0.099 to 0.629 min^{-2} as the carbaryl inlet concentration decreases from

Carbaryl Degradation in CSTR by AFT

J. Agric. Food Chem., Vol. 54, No. 26, 2006 **10065**

99.75 to 20.52 μM. Because the temperature, Fenton reagent delivery rate/ratio, and carbaryl feeding flow rate were invariant for these experiments, the parameters k_1, k_2, ϵ, ϕ, and v_0 should be constant. The only variable in the rate parameter k ($k = \lambda k_1 k_2 \epsilon \phi v_0^2$) is the average lifetime of $^\bullet$OH (λ). Therefore, the increase of carbaryl inlet concentration will result in a shorter lifetime of $^\bullet$OH, which is in agreement with the observation in the AFT batch reactor (7). The half-life time ($t_{1/2}$) of carbaryl can be obtained from the modeling simulation, which exhibits a good linear correlation with the carbaryl initial concentration as shown in eq 16.

$$t_{1/2} = 0.7436 + 0.01549C_0 \quad R^2 = 0.99 \quad (16)$$

On the other hand, the fitted shape parameter β is ~0.8 under different inlet concentrations, showing that β does not vary with carbaryl inlet concentration when other experimental conditions are fixed. This result indicates that the carbaryl inlet concentration does not affect the reactivity and availability of Fenton reagents and hydroxyl radicals.

By employing the proposed model, the predicted instantaneous degradation rate ($\mu = - dC/dt$) was plotted as a function of treatment time (t) as shown in **Figure 3b**. It is interesting to note that the instantaneous degradation rate (μ) in the evaluated system increases as the AFT proceeds during the early treatment stage, reaches a maximum instantaneous degradation rate (μ_{max}) within 5 min, and then declines continuously and eventually reaches zero when the system achieves the steady-state ($\mu = - dC/dt = 0$). Prior to reaching μ_{max}, μ increases at a similar rate ($\mu' = d\mu/dt$) at different concentration levels at a given time (inset of **Figure 3b**). The magnitude of μ_{max} and the time to reach μ_{max} were found to increase with increasing carbaryl inlet concentration. Although μ_{max} at higher concentrations was greater than that at lower concentrations, a quasi-steady-state (i.e., when μ is close to zero, but not zero) was achieved in a shorter time at lower concentration due to the less amount of carbaryl. Therefore, to meet the pesticide discharge requirement over a given time period, a stronger oxidation condition is required for a higher pesticide inlet concentration. Alternative methods to accelerate the degradation process will be discussed in later sections.

Effect of Ferrous ion Delivery Rate on Carbaryl Degradation. To investigate the effect of ferrous ion (Fe^{2+}) delivery rate on carbaryl degradation in CSTR by AFT, five current (I) levels (0.010. 0.020, 0.030, 0.040, and 0.050 A, corresponding to Fe^{2+} delivery rates of 15.6, 31.1, 46.7, 62.2, and 77.7 μM min^{-1}, respectively) were applied. At each current level, the H_2O_2 concentration was adjusted in order to achieve a fixed H_2O_2:Fe^{2+} ratio of 5:1. The carbaryl inlet concentration (C_0) and feeding rate (Q) were fixed at 100.50 μM and 7.5 mL min^{-1}, respectively. The observed carbaryl concentration profiles (**Figure 4a**) show that the higher the Fe^{2+} delivery rate is (higher current, I), the faster the carbaryl degradation is. When the Fe^{2+} delivery rate was as low as 15.67 μM min^{-1} ($I = 0.010$ A), <98% of carbaryl was removed after 1 h (data after 12 min not shown), whereas carbaryl was not detected within 2.5 min when the Fe^{2+} delivery rate was 77.7 μM min^{-1} ($I = 0.050$ A). This observation is consistent with carbaryl degradation in a batch AFT when the current was in the range of 0.010−0.100 A at an H_2O_2:Fe^{2+} ratio of 10:1 (8).

Applying the previously described modeling approach, the experimental data were found to follow the model prediction as shown in **Figure 4a** and **Table 3** ($R^2 \geq 0.993$). The fitted reaction rate parameter (k) increased from 0.027 to 0.798 min^{-2} as the Fe^{2+} delivery rate (v_0) increased from 15.6 to 77.7 μM min^{-1} (i.e., current increased from 0.010 to 0.050 A), which is
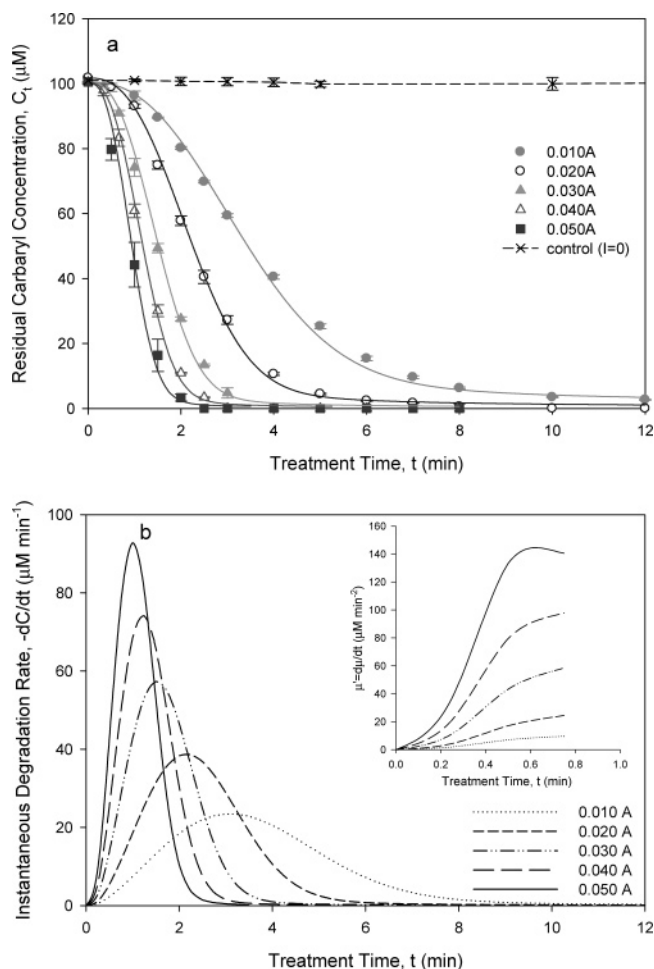

Figure 4. Effect of Fe^{2+} delivery rate (v_0) on carbaryl degradation in CSRT by AFT ($C_0 = 100.50$ μM, H_2O_2:$Fe^{2+} = 5$:1, and $Q = 7.5$ mL min^{-1}). (**a**) Modeling fit of experimental data (symbols represent experimental data, and lines represent model fit). (**b**) Model predicted instantaneous degradation rate as a function of treatment time; the inset is the $d\mu/dt$ vs treatment time curve.

consistent with the increase in the overall carbaryl degradation rate in this system. The increase of Fe^{2+} delivery into the system results in an increase of instantaneous Fe^{2+} concentration and Fe^{2+} average lifetime, which would be beneficial to the generation of $^\bullet$OH, and thus provides more potential opportunities for $^\bullet$OH to react with target pesticides. As for the shape parameter, β remains at a value of 0.8 when the current is $\geq$0.020 A. When the current is as low as 0.010 A (i.e., the concentration of both Fenton reactants is low), the shape parameter β is slightly lower (0.75), implying that the Fenton reagent reactivity and availability are very similar when $I \geq 0.020$ A, while slightly lower reactivity/availability results in carbaryl degradation at $I = 0.010$A.

The profiles of model-predicted instantaneous degradation rate herein display a similar shape as those discussed in the previous section. As illustrated in **Figure 4b**, the higher the Fe^{2+} delivery rate is (i.e., higher current), the less time needed to reach maximum degradation rate and quasi-steady-state and the greater the maximum degradation rate. In contrast to the similar increasing rate of μ at different carbaryl inlet concentrations, $d\mu/dt$ increases with increasing Fe^{2+} delivery rate at a given time (inset of **Figure 4b**). As a result, a higher Fe^{2+} delivery rate can accelerate the AFT process, but other factors, especially electricity cost, need to be considered when determining the optimal operating conditions in a practical application.
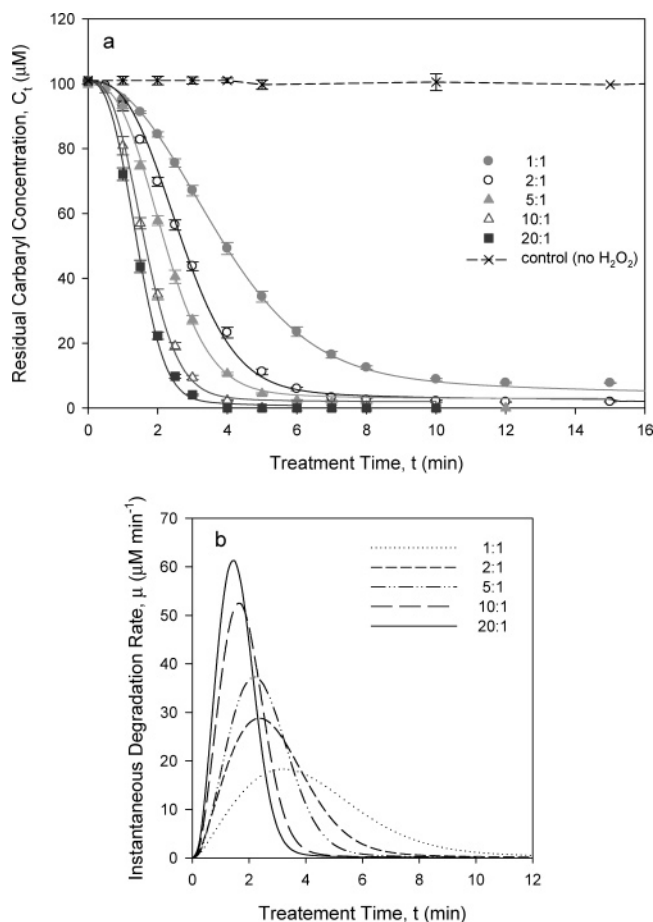
10066 *J. Agric. Food Chem.,* Vol. 54, No. 26, 2006

Kong and Lemley

Figure 5. Effect of H_2O_2:Fe^{2+} delivery ratio (1:1, 2:1, 5:1, 10:1, and 20:1) on carbaryl degradation in CSRT by AFT ($C_0 = 100.75$ μM, $I = 0.020$ A, and $Q = 7.5$ mL min^{-1}). (**a**) Modeling fit of experimental data (symbols represent experimental data, and lines represent model fit). (**b**) Model predicted instantaneous degradation rate as a function of treatment time.

Effect of H_2O_2:Fe^{2+} Delivery Ratio on Carbaryl Degradation. The carbaryl inlet concentration and feeding rate were fixed at 100.75 μM and 7.5 mL min^{-1}, respectively, and the current was 0.020 A, while the initial concentration of H_2O_2 varied at 0.0144, 0.0288, 0.0620, 0.1240, and 0.2480 M in order to achieve five different H_2O_2:Fe^{2+} delivery ratios of 1:1, 2:1, 5:1, 10:1, and 20:1, respectively. As shown in **Figure 5a**, the carbaryl degradation rate increased with increasing H_2O_2:Fe^{2+} ratio; that is, the higher H_2O_2:Fe^{2+} ratio favors carbaryl degradation over the range of 1:1 to 20:1. At an H_2O_2:Fe^{2+} ratio of 1:1, only 92% percent of the carbaryl was degraded after 1 h of treatment (data after 15 min not shown), and for the ratio of 2:1, the maximum removal of carbaryl was ~98% after an hour. However, no carbaryl was detected in the effluent after 4 min when the H_2O_2:Fe^{2+} ratio was at 20:1. Previous work on batch AFT in our laboratory also showed an increase in carbaryl degradation rate as the H_2O_2:Fe^{2+} ratio was increased from 1:1 to 15:1 (8).

Figure 5a displays a very good fit between the derived model and the observed data ($R^2 \geq 0.998$). The fitted reaction rate parameter (k) increased from 0.012 to 0.291 min^{-2} as the H_2O_2:Fe^{2+} ratio varied from 1:1 to 20:1 (**Table 4**). However, the increasing range of k (0.012–0.029 min^{-2}) is narrower as compared to the range when the current (I) increased from 0.010 to 0.050 A (0.027–0.798 min^{-2}), indicating that the Fe^{2+} delivery rate is a more significant factor than H_2O_2:Fe^{2+} ratio under the evaluated experimental conditions. This can be explained by the fact that in most of the experiments the

Table 3. Modeling of Carbaryl Degradation under Different Fe^{2+} Delivery Rate in CSTR by AFT

current, I (A)	Fe^{2+} delivery rate, v_0 (μM min^{-1})	k (min^{-2})	β	R^2
0.010	15.6	0.027 ± 0.002	0.75 ± 0.01	0.998
0.020	31.1	0.096 ± 0.004	0.80 ± 0.01	0.998
0.030	46.7	0.241 ± 0.007	0.79 ± 0.01	0.998
0.040	62.2	0.454 ± 0.007	0.80 ± 0.01	0.999
0.050	77.7	0.798 ± 0.007	0.79 ± 0.01	0.993

Table 4. Modeling of Carbaryl Degradation under Different H_2O_2:Fe^{2+} Delivery Ratio in CSTR by AFT

H_2O_2:Fe^{2+} ratio	k (min^{-2})	β	R^2
1:1	0.012 ± 0.004	0.59 ± 0.01	0.999
2:1	0.038 ± 0.002	0.70 ± 0.01	0.999
5:1	0.089 ± 0.004	0.80 ± 0.01	0.998
10:1	0.195 ± 0.011	0.79 ± 0.01	0.998
20:1	0.291 ± 0.007	0.80 ± 0.01	0.998

concentration of H_2O_2 is stoichiometrically much higher than that of Fe^{2+}; therefore, the Fe^{2+} concentration is the determining factor. The rate parameter increase is also consistent with the overall carbaryl degradation rate, which increased with the increasing H_2O_2:Fe^{2+} ratio. The shape parameter (β) is 0.6 and 0.7 when the H_2O_2:Fe^{2+} ratio is 1:1 and 2:1, respectively, whereas it remains at 0.8 when the ratio is great than 2:1. It is well-established that the Fenton reaction is more efficient at higher H_2O_2:Fe^{2+} ratios, due to extraneous reactions of H_2O_2 with species other than Fe^{2+}. When the reaction is less efficient at the lower ratios, the Fenton reagent reactivity and availability are most likely lower. The result of a smaller shape parameter with lower ratio of H_2O_2:Fe^{2+} is consistent with the previous finding that β is affected by a low Fenton reagent delivery rate, which is also related to the reduction of Fenton reagent reactivity/availability. When the Fe^{2+} delivery rate and H_2O_2:Fe^{2+} ratio are >15.6 μM min^{-1} and 2:1, respectively, β does not change.

The instantaneous degradation rate profiles are very similar to those with different Fe^{2+} delivery rates; that is, the higher the H_2O_2:Fe^{2+} ratio is, the faster it is to achieve μ_{max} and quasi-steady-state. In addition, the magnitude of μ_{max} increases with H_2O_2:Fe^{2+} ratio. Therefore, over the range of 1:1 to 20:1, a higher H_2O_2:Fe^{2+} ratio will provide a stronger oxidation condition for the target pesticides in AFT. However, the effectiveness of H_2O_2:Fe^{2+} ratio and Fe^{2+} delivery rate to pesticide degradation could be different, depending not only on the degradation rate but also on the cost of Fenton reagent and electricity.

Effect of Carbaryl Feeding Flow Rate on Its Degradation. To evaluate the effect of the carbaryl feeding flow rate (Q) on carbaryl degradation in CSTR by AFT, carbaryl was fed into the anodic half-cell at five different flow rates (2.6. 5.1, 7.5, 10.0, and 14.6 mL min^{-1}). The other experimental conditions were as follows: $I = 0.020$ A, H_2O_2:$Fe^{2+} = 5:1$, and $C_0 = 99.75$ μM. The carbaryl concentration profiles at different carbaryl feeding rates are shown in **Figure 6a**. At a flow rate of 14.6 mL min^{-1}, approximately 94% of the carbaryl was removed after 1 h of treatment (data after 12 min not shown). Carbaryl degraded slightly faster at lower flow rates than at higher ones. Under the evaluated experimental conditions, it was observed that the flow rate played an insignificant role in carbaryl degradation.

The developed model simulates the obtained experimental data very well (**Table 5**), with R^2 values ≥ 0.998. The k values
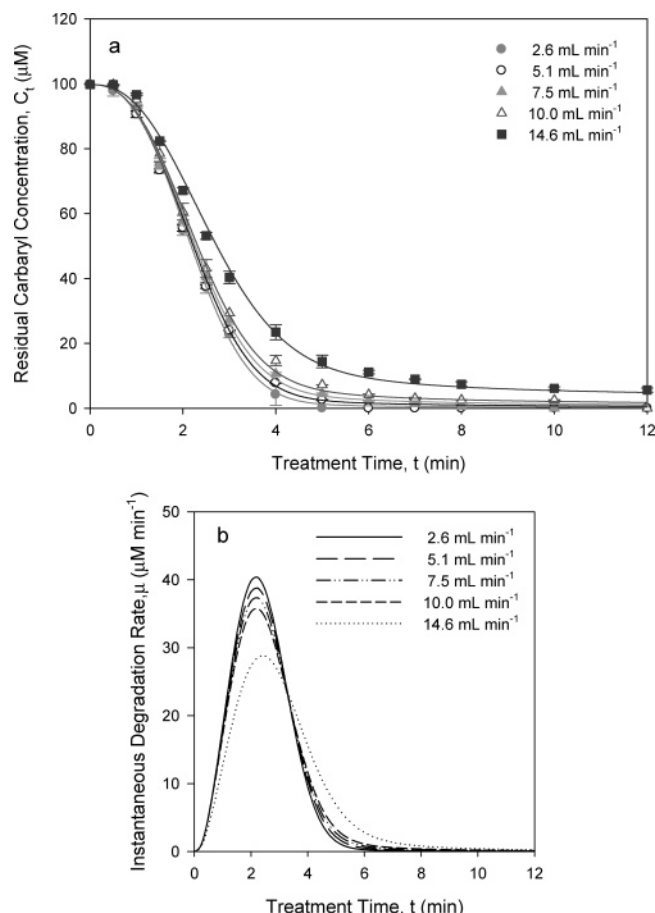
Carbaryl Degradation in CSTR by AFT

J. Agric. Food Chem., Vol. 54, No. 26, 2006 **10067**

Figure 6. Effect of carbaryl feeding flow rate (Q) on carbaryl degradation in CSRT by AFT ($C_0 = 99.75 \ \mu$M, $I = 0.020$ A, and H_2O_2:Fe^{2+} = 5:1). (**a**) Modeling fit of experimental data (symbols represent experimental data, and lines represent model fit). (**b**) Model predicted instantaneous degradation rate as a function of treatment time.

Table 5. Modeling of Carbaryl Degradation under Different Carbaryl Feeding Rates in CSTR by AFT

carbaryl feeding rate (mL min^{-1})	k (min^{-2})	k/q^2	β	R^2
2.63 ± 0.04	0.058 ± 0.002	103.0	0.79 ± 0.01	0.999
5.08 ± 0.02	0.075 ± 0.002	36.0	0.78 ± 0.01	0.998
7.50 ± 0.04	0.089 ± 0.002	19.0	0.80 ± 0.01	0.998
10.30 ± 0.04	0.099 ± 0.005	12.0	0.79 ± 0.01	0.998
14.61 ± 0.10	0.102 ± 0.002	3.9	0.80 ± 0.01	0.997

Figure 7. Modeling of selected pesticide degradations in CSRT by AFT ($C_0 \cong 100 \ \mu$M, $I = 0.020$ A, H_2O_2:Fe^{2+} = 5:1, and $Q = 7.5$ mL min^{-1}). (**a**) Modeling fit of experimental data (symbols represent experimental data, and lines represent model fit). (**b**) Model predicted instantaneous degradation rate as a function of treatment time.

Table 6. Modeling of Various Pesticide Degradations in CSTR by AFT

pesticides	k (min^{-2})	β	R^2
alachlor	0.068 ± 0.002	0.60 ± 0.01	0.992
carbaryl	0.090 ± 0.002	0.80 ± 0.01	0.998
carbofuran	0.019 ± 0.002	0.54 ± 0.01	0.996
diazinon	0.125 ± 0.003	0.59 ± 0.01	0.994
metolachlor	0.055 ± 0.002	0.59 ± 0.01	0.998
2,4-D	0.125 ± 0.002	0.70 ± 0.01	0.994

exhibited a slight increase when the flow rate increased from 2.6 to 14.6 mL min^{-1}, which is probably due to the reduced retention time of the Fenton reagent with flow rate increase. The shape parameter β does not change over the evaluated flow rate range, indicating that flow rate has no influence on the reactivity and availability of Fenton reagents and hydroxyl radicals. From the instantaneous degradation rate vs time curves, it can be observed that the time to achieve the maximum degradation rate (μ_{max}) is similar at a different flow rate, whereas the value of μ_{max} increases and the time needed to reach quasi-steady-state decreases as the flow rate increases (**Figure 6b**). The rate parameter values at different flow rates do not correlate with the overall carbaryl degradation rate, which decreases with increasing flow rate as shown in **Figure 6a**. This result could be attributed to the fact that the flow rate is an independent variable influencing the overall degradation rate. However, the reaction rate parameter does not reflect all of the impact of flow rate on carbaryl degradation. The dimensionless parameter k/q^2
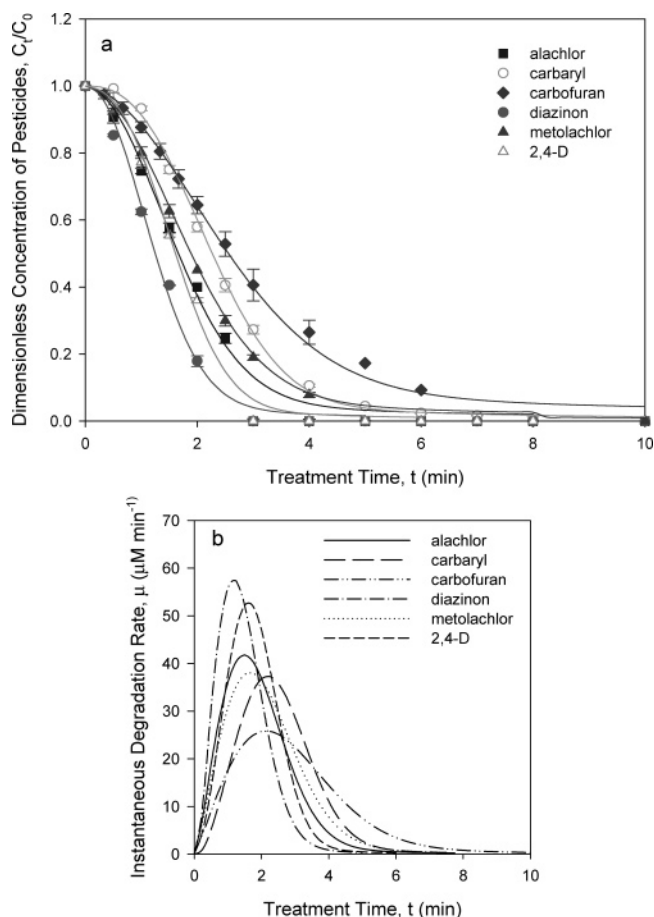
decreased from 103.0 to 3.9 as the flow rate increased from 2.6 to 14.6 mL min^{-1}, which is consistent with the overall carbaryl degradation rate. On the basis of the above discussion, the reaction rate parameter (k) can be a good indicator of the degradation rate for a given pesticide at a given flow rate. However, when the flow rate varies, the dimensionless parameter k/q^2 better tracks the pesticide degradation process.

Degradation Kinetic Model Application to Other Pesticides. To validate the proposed model application to other pesticides, the degradations of alachlor, carbaryl, carbofuran, diazinon, metolachlor, and 2,4-D were investigated at an inlet concentration of approximately 100 μM, feeding flow rate of 7.5 mL min^{-1}, current of 0.020 A, and an H_2O_2:Fe^{2+} ratio of 5:1. As shown in **Figure 7a**, the degradation rates can be visually determined to be in the following order: diazinon > 2,4-D > alachlor > metolachlor > carbaryl > carbofuran. This order can partially be confirmed by comparing with available
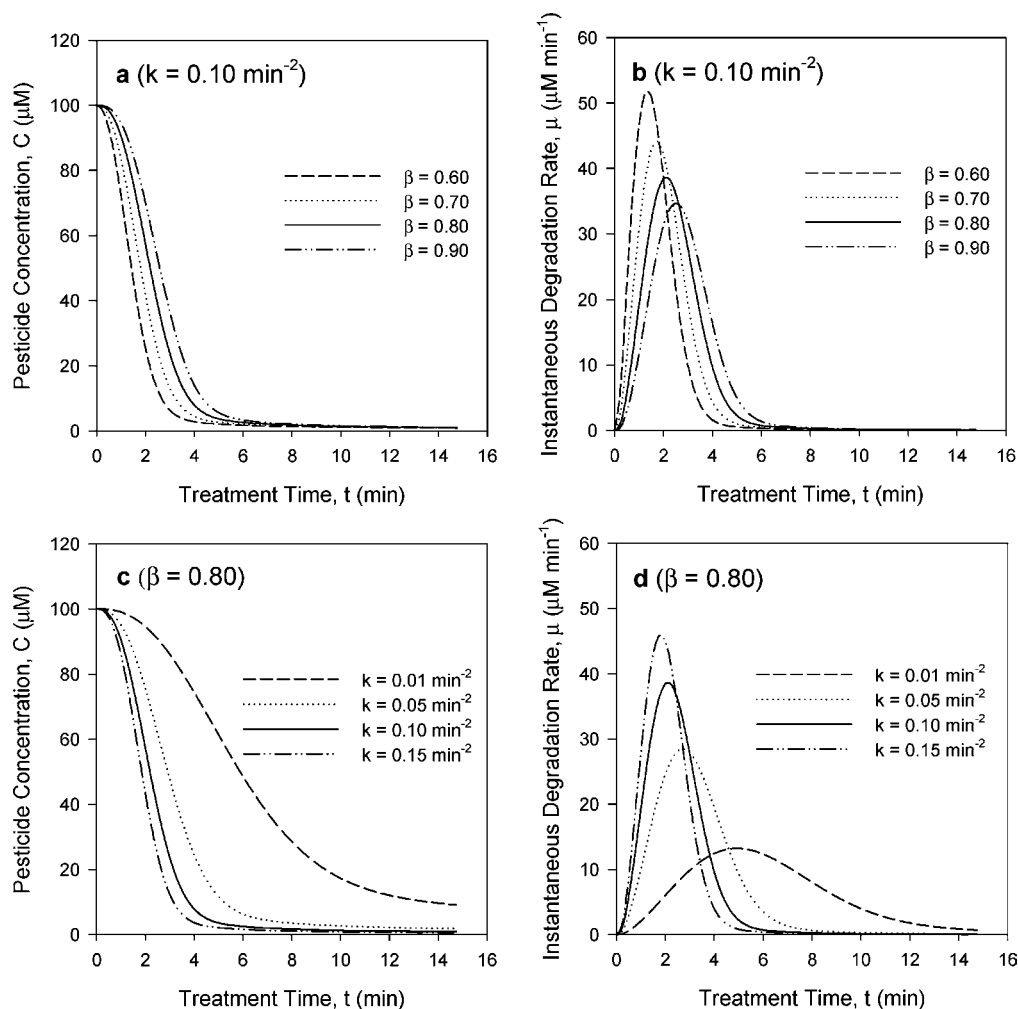
Figure 8. Representative sensitivity analysis of fitting parameters (k and β) on pesticide degradation rate. (**a**) Pesticide concentration profile at different β values (0.6, 0.7, 0.8, and 0.9); $k = 0.10$ min^{-2}. (**b**) Pesticide degradation rate profile at different β values (0.6, 0.7, 0.8, and 0.9); $k = 0.10$ min^{-2}. (**c**) Pesticide concentration profile at different k values (0.01, 0.05, 0.10, and 0.15 min^{-2}); $\beta = 0.80$. (**d**) Pesticide degradation rate profile at different k values (0.01, 0.05, 0.10, and 0.15 min^{-2}); $\beta = 0.80$.

published data of batch AFT (*7−9, 15*). However, it cannot be obtained directly from either the rate parameter, k (or dimensionless parameter, k/q^2), or the shape parameter, β (**Table 6**). When the shape parameters are the same, the higher k value obviously indicates a higher degradation rate; for example, alachlor degraded slightly faster than metolachlor. When the k values are similar, a low β value reflects a faster degradation. For example, diazinon and 2, 4-D have the same k value of 1.25 min^{-2}, whereas the shape parameter of diazinon (0.6) is much lower than that of 2,4-D (0.7) and results in a faster degradation. This result sounds contrary to the previous observation that low β values at low Fe^{2+} delivery ratio or H_2O_2:Fe^{2+} ratio relate to a lower degradation rate. However, when comparing the shape parameter of different pesticides, a small β value may indicate less reactivity or availability of Fenton reagents but does not necessarily result in a slower consumption of ·OH by the target pesticide. In addition, although the shape parameter β was introduced by simulating the Fenton reagent concentration profiles, it does not mean that β is independent of the pesticide. Because of their different chemical structures, pesticides could have different interactions with the Fenton reagents and/or Fenton reaction products including Fe^{3+} and ·OH. These interactions may alter the availability of Fenton reagents participating in a ·OH-generating reaction and the consumption rate of ·OH by a certain pesticide. For example, in a previous batch AFT study, the degradation kinetics of

metribuzin and triazinone/triazine herbicides was different from that of the original AFT kinetic model. The formation of a weak complex between metribuzin or other triazinone/triazine herbicides and Fe^{3+} via the "N" on the ring in the pesticide was considered to be responsible for the different kinetic model (*29*). However, how the β in the newly developed model relates to a specific pesticide is not very clear at present and needs to be evaluated on the basis of a wider variety of pesticides in future studies. β is not recommended for use as an independent indicator of the degradation rate.

Overall, it is appropriate to compare the degradation rate of various pesticides when either k or β is similar. When both the k and the β values are different, such as alachlor and carbaryl or metolachlor and carbaryl, it is hard to compare the degradation rate by comparing the fitting parameters (k and β). Under this circumstance, the degradation rate can be compared by either the observed pesticide concentration profile or the model-predicted instantaneous degradation rate vs time curve. As shown in **Figure 7b**, the time needed to reach the quasi-steady-state/maximum degradation rate and the value of maximum degradation rate exhibit an order similar to that obtained from the concentration profile.

To better understand the effect of the fitting parameters (k and β) on the degradation rate, sensitivity analyses were performed. On the basis of the modeling analysis in previous sections, k can vary from 0.01 to 0.80 min^{-2}, whereas β is

mostly likely in the range of 0.5−0.8 under evaluated experimental conditions. As an example, $k = 0.10$ min^{-2} and $\beta = 0.80$ were selected as two typical values of the corresponding fitting parameter. Two representative cases of sensitivity analysis are presented as follows: (i) β varied from 0.6 to 0.9 with $k = 0.10$ min^{-2} (**Figure 8a,b**) and (ii) k varied from 0.01 to 0.15 min^{-2}, with $\beta = 0.80$ (**Figure 8c,d**). Comparing case i with case ii, it is obvious that the pesticide degradation rate is more sensitive to k values than to β over the evaluated parameter range, as seen in both the pesticide concentration and the instantaneous degradation rate profiles.

The developed kinetic-based semiempirical model has been shown to provide important information on a single pesticide degradation in a well-defined CSTR by AFT. However, to adapt the model to actual pesticide wastewater, more factors need to be considered in future research, such as the effect of other components in pesticide formulation (i.e., surfactants, solvents, etc.), pesticide mixtures, natural organic matter, bicarbonate or carbonate, etc.

ACKNOWLEDGMENT

LITERATURE CITED

(1) Felsot, A. S.; Racke, K. D.; Hamilton, D. J. Disposal and degradation of pesticide waste. *Rev. Environ. Contam. Toxicol.* **2003**, *177*, 123−200.

(2) Muller, K.; Bach, M.; Hartmann, H.; Spiteller, M.; Frede, H.-G. Point-and nonpoint-source pesticide contamination in the Zwester Ohm Catchment, Germany. *J. Environ. Qual.* **2002**, *31*, 309−318.

(3) Peris-Cardells, E.; Terol, J.; Mauri, A. R.; de la Guardia, M.; Pramauro, E. Continuous flow photocatalytic degradation of carbaryl in aqueous media. *J. Environ. Sci. Health B* **1993**, *28*, 431−445.

(4) Pignatello, J. J.; Baehr, K. Ferric complexes as catalysts for "Fenton" degradation of 2,4-D and metolachlor in soil. *J. Environ. Qual.* **1994**, *23*, 365−370.

(5) Rivas, F. J.; Navarrete, V.; Beltran, F. J.; Garcia-Araya, J. F. Simazin Fenton's oxidation in a continuous reactor. *Appl. Catal. B* **2004**, *48*, 249−258.

(6) Chan, K. H. C. W. Modeling the reaction kinetics of Fenton's process on the removal of atrazine. *Chemosphere* **2003**, *51*, 305−311.

(7) Wang, Q.; Lemley, A. T. Kinetic model and optimization of 2,4-D degradation by anodic Fenton treatment. *Environ. Sci. Technol.* **2001**, *35* (22), 4509−4514.

(8) Wang, Q.; Lemley, A. T. Oxidation of carbaryl in aqueous solution by membrane anodic Fenton treatment. *J. Agric. Food Chem.* **2002**, *50* (8), 2331−2337.

(9) Wang, Q.; Lemley, A. T. Competitive degradation and detoxification of carbamate insecticides by membrane anodic Fenton treatment. *J. Agric. Food Chem.* **2003**, *51* (18), 5382−5390.

(10) Komives, C.; Osborne, D.; Russell, A. J. Degradation of pesticides in a continouse-flow two-phase microemulsion reactor. *Biotechnol. Prog.* **1994**, *10*, 340−343.

(11) Chiron, S.; Fernandez-Alba, A.; Rodriguez, A.; Garcia-Calvo, E. Pesticide chemical oxidation: State-of-the-art. *Water Res.* **2000**, *34* (2), 366−377.

(12) Watts, R. J.; Teel, A. L. Chemistry of modified Fenton's reagent (catalyzed H$_2$O$_2$ propagations-CHP) for in situ soil and groundwater remediation. *J. Environ. Eng.* **2005**, *131* (4), 612−622.

(13) Buxton, G. V.; Greenstock, C. L.; Helman, W. P.; Ross, A. B. Critical review of rate constants for reactions of hydrated electrons, hydrogen atoms and hydroxyl radicals (•OH/•O$^-$) in aqueous solution. *J. Phys. Chem. Ref. Data* **1988**, *17*, 513−886.

(14) Wang, Q.; Scherer, E. M.; Lemley, A. T. Metribuzin degradaton by membrane anodic Fenton treatment and its interacton with ferric ion. *Environ. Sci. Technol.* **2003**, *38* (4), 1221−1227.

(15) Wang, Q.; Lemley, A. T. Oxidation of diazinon by anodic Fenton treatment. *Water Res.* **2002**, *36*, 3237−3244.

(16) Wang, Q.; Lemely, A. T. Oxidative degradation and detoxification of aqueous carborfuran by membrane anodic Fenton treatment. *J. Hazard. Mater.* **2003**, *B98*, 241−255.

(17) Friedman, C. L.; Lemely, A. T.; Hay, A. Degradation of chloroacetanilide herbicides by anodic Fenton treatment. *J. Agric. Food Chem.* **2006**, *54*, 2640−2651.

(18) Wang, Q.; Lemley, A. T. Competitive degradation and detoxification of carbamate insecticides by membrane anodic Fenton treatment. *J. Agric. Food Chem.* **2003**, *51*, 5382−5390.

(19) Worek, F.; Szinicz, L.; Eyer, P.; Thiermann, J. Evaluation of oxime efficacy in nerve agent poisoning: Development of a kinetic-based dynamic model. *Toxicol. Appl. Pharmacol.* **2005**, *209*, 193−202.

(20) Duirk, S. E.; Collett, T. W. Degradation of chlorpyrifos in aqueous chlorine solutions: Pathways, kinetics, and modeling. *Environ. Sci. Technol.* **2006**, *40*, 546−551.

(21) Lin, S.-S.; Gurol, M. D. Catalytic decomposition of hydrogen peroxide on iron oxide: Kinetics, mechanism, and implications. *Environ. Sci. Technol.* **1998**, *32* (10), 1417−1423.

(22) *Standard Methods for the Examination of Water and Wastewater*, 20th ed.; American Public Health Association, American Water Works Association and Water Environment Federation: Washington, DC, 1998.

(23) Huckaba, C. E.; Keyes, F. G. The accuracy of estimation of hydrogen peroxide by potassium permanganate titration. *J. Am. Chem. Soc* **1948**, *70*, 1640.

(24) Systat Software Inc. *SigmaPlot 9.01*; Systat Software Inc.

(25) Walling, C. Fenton's reagent revisitied. *Acc. Chem. Res.* **1975**, *8*, 125−131.

(26) Rush, J. D.; Bielski, B. H. Pulse radiolytic studies of the reactions of HO$_2$/O$_2^-$ with Fe (II)/Fe(III) ions. The reactivity of HO$_2$/O$_2^-$ with ferric ions and its implication on the occurrence of Haber-Weiss reaction. *J. Phys. Chem.* **1985**, *89*, 5602−5066.

(27) Stuglik, Z.; Zagorski, Z. P. Pulse radiolysis of neutral iron(II) solutions: Oxidation of ferrous ions by OH racicals. *Radiat Phys. Chem.* **1981**, *17*, 229−233.

(28) Sehested, K.; Rasmussen, O. L.; Ficke, H. Rate constant of OH with HO$_2$, O$_2^-$ and H$_2$O$_2^+$ from hydrogen peroxide in pulse-irradiated oxygenated water. *J. Phys. Chem.* **1968**, *72*, 626−631.

(29) Wang, Q.; Scherer, E. M.; Lemley, A. T. Metribuzin degradation by membrane anodic Fenton treatment and its interaction with ferric ion. *Environ. Sci. Technol.* **2004**, *38*, 1221−1227.